A PROOF OF THE KASHAEV SIGNATURE CONJECTURE

by

Jessica Chengjin Liu

A thesis submitted in conformity with
the requirements for the degree of
Doctor of Philosophy

Graduate Department of Mathematics
University of Toronto

ABSTRACT

A Proof of the Kashaev Signature Conjecture

Jessica Chengjin Liu

Doctor of Philosophy

Graduate Department of Mathematics

University of Toronto

2025

The Levine-Tristram signature is a well-known invariant of links that is topological in nature – its known definitions rely on manifolds associated with the link and it is related to other topological invariants such as genus, unlinking number, and the Alexander polynomial. In 2018 Kashaev introduced a link invariant defined using a simple algorithm on link diagrams which he conjectured also computes the Levine-Tristram signature [Kas21]. In this thesis we present a method of obtaining Kashaev's invariant using the original Seifert surface definition of the Levine-Tristram signature, making evident the relationship between the two and thereby proving Kashaev's conjecture. We obtain as a corollary another formula for the Alexander polynomial. The content of this thesis is based on [Liu25].

ACKNOWLEDGEMENTS

My sincerest gratitute to my supervisor Dror Bar-Natan, who has invested an unbelievable amount of time and energy in me over the last five years. I am incredibly lucky to have had the opportunity to know and to work with Dror.

I am also grateful to the many kind people who have provided me with their support and guidance. A special thanks to Zsuzsanna Dancso, Nancy Scherich, and Anthony Conway, who have been especially generous with their time and knowledge.

I also wish to thank my collaborators David Cimasoni and Livio Ferretti for the pleasure of working with them, as well as Rinat Kashaev for many fruitful conversations.

A final acknowledgement to my friends and family, to whom I'm grateful for everything.

CONTENTS

1

PRELIMINARIES

Before discussing invariants of links, we first discuss links themselves.

Definition 1.1. An **(n-component) link** is an embedding $L : \sqcup_n S^1 \to S^3$ modulo ambient isotopy of S^3.

One might find slightly different definitions in other sources – for example, some might require the map to be smooth or piecewise linear – but these differences do not affect the content of this thesis. For convenience we use the term *link* for both the embedding and its image. Below we introduce some additional relevant terminology.

1. A **component** of a link refers to the restriction to a single copy of S^1, or to the image of such a restriction. A **(k-component) sublink** of an n-component link is a restriction to some subset $\sqcup_k S^1 \subseteq \sqcup_n S^1$. A 1-component link is a **knot**.

2. An **oriented link** is a link with a choice of orientation on each copy of S^1. Two oriented links are considered equivalent if the ambient isotopy preserves orientation. The **reverse** rL of an oriented link L is the link with the opposite choice of orientation on each component.

3. The **disjoint union** $L_1 \sqcup L_2$ of two links L_1 and L_2 is the link consisting of L_1 and L_2 as sublinks lying on different sides of an embedded S^2 in S^3.

Consider a projection of a link onto a plane so that at most two points project to the same point. A **link diagram** is a picture representing such a projection, together with information about which point is “above" the other when two points overlap in the projection – such overlapping points are called **crossings**. The orientation on a diagram for an oriented link is denoted by arrows on the strands. Near a crossing, the orientation determines the **sign** of the crossing, see Figure 1.1.

Figure 1.1: A **positive** (+1) crossing (left) and a **negative** (-1) crossing (right).

Two diagrams represent the same link if and only if one can be brought to the other by a sequence of modifications to the diagram known as **Reidemeister moves**. Constructing a sequence of moves therefore proves that two diagrams represent the same link. But given two diagrams (or two descriptions of any kind), how can we show that they represent different links?

A **link invariant** is a function whose domain is links; if two diagrams evaluate to different values under some invariant, then they must represent different links. One way to define a link invariant is by defining a function on diagrams and showing that it doesn't change under Reidemeister moves. The Kashaev invariant, see Theorem 2.3, is defined in this diagrammatic fashion. Another way to define link invariants is by considering the topology surrounding the link. The Levine-Tristram signature and the Alexander polynomial are two invariants that admit such topological definitions. The crux of this thesis is Theorem 3.1, which shows that the diagrammatic Kashaev invariant computes the same thing as the topological Levine-Tristram signature.

The remainder of this chapter focuses on defining the Levine-Tristram signature and the Alexander polynomial using Seifert matrices. The content we present can be found in almost any introductory textbook on knot theory, for example [Lic], which serves as our main reference for this chapter.

1.1 SEIFERT SURFACES AND MATRICES

One way to define both the Levine-Tristram signature and the Alexander polynomial is by using Seifert surfaces and Seifert matrices.

Definition 1.2. A **Seifert surface** for an oriented link L is a compact, oriented surface embedded in S^3 that has no closed components and whose boundary is L.

Remark 1.3. Many definitions of Seifert surface require that it be connected; we only require that it has no closed components. Connectivity is not required to define the Levine-Tristram signature, though it is required to define the Alexander polynomial. We specify connectivity as needed.

Every link admits a Seifert surface. One way to show this is via Seifert's algorithm, which is used explicitly in the proof of Theorem 3.1.

Definition 1.4. Let D be a diagram for an oriented link L. The following process is **Seifert's algorithm**, which constructs a Seifert surface for L using D.

1. Modify the crossings of D as in Figure 1.2 to get a diagram consisting of a disjoint union of simple closed curves.

Figure 1.2: Modification of a positive crossing (left) and a negative crossing (right).

2. For each closed curve, add in a disk that lies below the plane so that the boundary of the disk is the curve. Let the disks be disjoint and let their orientations be induced by the orientations of their boundaries.

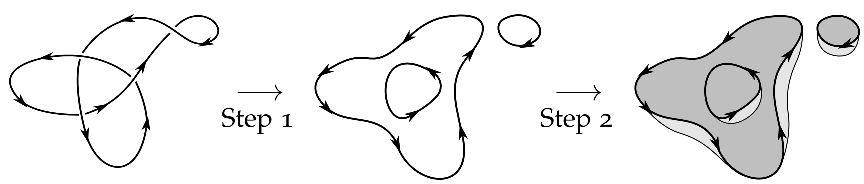

Figure 1.3: Step 1: Modifying crossings to get a disjoint union of simple closed curves. Step 2: Adding in disjoint disks bounded by the simple curves. The dark grey side is positive and the light grey side is negative.

3. Add twisted strips between the disks at the locations where the crossings of D originally were so that the boundaries of the strips are the crossings. The direction of the twist depends on the sign of the crossing.

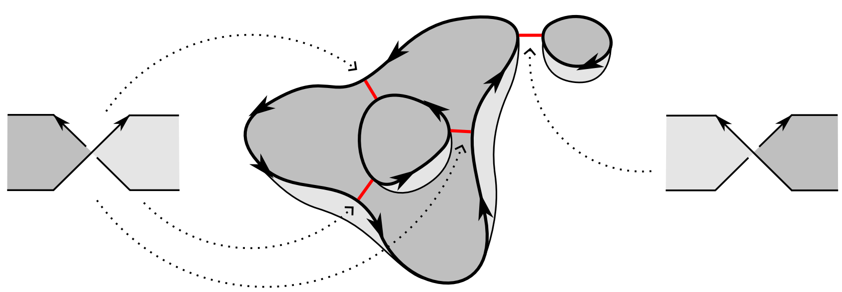

Figure 1.4: Adding in twisted strips where the crossings used to be (red).

One can verify that the resulting surface is indeed a Seifert surface for L.

In order to define Seifert matrices we also need the notion of linking number.

Definition 1.5. Consider two sublinks L_1 and L_2 of a link that don't share any components. The **linking number** between L_1 and L_2, denoted $\mathrm{lk}(L_1, L_2)$, is half the sum of the signs of crossings where one strand is from L_1 and the other is from L_2 in a diagram of the link.

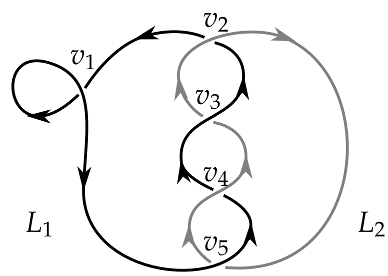

Figure 1.5: The four crossings between L_1 and L_2 are v_2, v_3, v_4, and v_5. They all have sign $+1$ so $\mathrm{lk}(L_1, L_2) = \frac{1}{2}(4) = 2$.

One can show that linking number is independent of the diagram used by showing that it is invariant under Reidemeister moves, see [Lic].

Remark 1.6. If L_1 is a 1-component link (i.e. a knot), then $\mathrm{lk}(L_1, L_2) = [L_2] \in H_1(S^3 \setminus L_1) \cong \mathbb{Z}$, given an appropriate choice of orientation.

Definition 1.7. Let Σ be a Seifert surface for an oriented link L, and consider a regular neighbourhood of Σ homeomorphic to $\Sigma \times [-1, 1]$, where Σ is identified with $\Sigma \times \{0\}$. Let $i^- : H_1(\Sigma; \mathbb{Z}) \to H_1(S^3 \setminus \Sigma; \mathbb{Z})$ denote a pushoff in the negative direction, which sends the homology class of a curve γ to that of $\gamma \times \{-1\}$. The **Seifert form** of Σ is the bilinear form on $H_1(\Sigma)$ given by

$$\begin{aligned} H_1(\Sigma) \times H_1(\Sigma) &\to \mathbb{Z} \\ (a, b) &\mapsto \mathrm{lk}(i^{-1}(a), b) \end{aligned}$$

on primitive classes and extending linearly to all of $H_1(\Sigma)$, where lk denotes the linking number.

Definition 1.8. A **Seifert matrix** is any matrix which represents the Seifert form.

Neither the Seifert matrix nor the Seifert form are link invariants. Indeed, the Seifert matrix depends on a choice of basis and the Seifert form depends on the Seifert surface, which always exists but is not unique to a given link – for example, we can always obtain a new surface from an existing one by performing a 0-surgery along an embedded arc.

Ambient isotopy and such surgeries are the only ways that any two Seifert surfaces can differ and these differences correspond to certain matrix moves on the Seifert matrix. Two matrices that differ by these matrix moves and basis changes are called **S-equivalent**, so that a well-defined invariant on S-equivalence classes of Seifert matrices is a well-defined invariant of links. Both the Levine-Tristram signature and the Alexander polynomial can be defined as invariants on S-equivalence classes. For proofs of the claims in this section and a more explicit description of S-equivalence, we refer to [Lic].

1.2 THE LEVINE-TRISTRAM SIGNATURE

The core of this thesis is the equation in Theorem 3.1, which features the Levine-Tristram signature on one side and the Kashaev matrix, introduced in Chapter 2, on the other. In this section we define the Levine-Tristram signature using Seifert matrices. For more details on the Levine-Tristram signature, see [Con21].

For any matrix A and complex unit number $\omega \in S^1$, the matrix $(1-\omega)A + (1-\overline{\omega})A^T$ is Hermitian and therefore has a well-defined signature: the number of positive eigenvalues minus the number of negative eigenvalues.

Definition 1.9. The **Levine-Tristram signature** of an oriented link $L \in S^3$ is the map $\sigma_L : S^1 \setminus \{1\} \to \mathbb{Z}$ given by

$$\sigma_L(\omega) = \operatorname{sign}((1-\omega)A + (1-\overline{\omega})A^T)$$

where A is any Seifert matrix for L and sign denotes the signature.

One can show that this is well-defined using S-equivalence, see [Lic]. The Levine-Tristram signature evaluated at $\omega = -1$ is the classical signature (or simply, signature).

The signature of a Hermitian matrix does not change if the matrix is enlarged by adding a row and column of zeros, thus the Seifert matrix A in the definition of σ_L need not be taken with respect to a basis of $H_1(\Sigma)$, but rather any set of generators. This is significant in the proof of Theorem 3.1.

By examining the definitions, one sees that the Levine-Tristram signature behaves well under basic operations on links and on ω. The properties in the following proposition are used in Chapter 3.

Proposition 1.10. *Let L be an oriented link and $\omega \in S^1 \setminus \{1\}$. The Levine-Tristram signature satisfies the following:*

1. *Symmetric under complex conjugation: $\sigma_L(\omega) = \sigma_L(\overline{\omega})$*

2. *Invariant under orientation reversal:* $\sigma_L(\omega) = \sigma_{rL}(\omega)$
3. *Additive under disjoint union:* $\sigma_{L' \sqcup L''}(\omega) = \sigma_{L'}(\omega) + \sigma_{L''}(\omega)$
4. *Additive under connected sum:* $\sigma_{L'\#L''}(\omega) = \sigma_{L'}(\omega) + \sigma_{L''}(\omega)$ *where* $L'\#L''$ *denotes a link obtained by performing a connected sum between any component of* L' *and any component of* L''

Proof. The first assertion is immediate by Definition 1.9 since the signature of a Hermitian matrix is invariant under complex conjugation. The second assertion is true because reversing the orientation on the link reverses the orientation of the Seifert surface and changes a Seifert matrix to its transpose. For the third and fourth assertions, note that $\begin{pmatrix} A' & 0 \\ 0 & A'' \end{pmatrix}$ is a Seifert matrix for both $L' \sqcup L''$ and $L'\#L''$ if A' and A'' are Seifert matrices for L' and L''. □

1.3 THE ALEXANDER POLYNOMIAL

As the Levine-Tristram signature is closely related to the Alexander polynomial, it is not surprising that the Kashaev matrix is also related to the Alexander polynomial, see Corollary 3.3.

We begin this section by introducing the Alexander module, though the definition of the Alexander polynomial can be understood independently using only the computation in Proposition 1.13.

Definition 1.11. Let L be an n-component link. The map

$$\begin{aligned} \pi_1(S^3 \setminus L) &\to \mathbb{Z} \cong \langle t \rangle \\ [\gamma] &\mapsto \operatorname{lk}(\gamma, L) \end{aligned}$$

induces a normal cover of $S^3 \setminus L$. The **Alexander module** of L is the first homology group of this cover equipped with a $\mathbb{Z}[t, t^{-1}]$-module structure given by the covering transformation.

Definition 1.12. The **Alexander polynomial** $\Delta_L(t)$ of a link L is a generator of the first elementary ideal of the Alexander module of L.

This definition of the Alexander polynomial is not always practical; one way to actually compute it is by using Seifert matrices.

Proposition 1.13. *The Alexander polynomial can computed by*

$$\Delta_L(t) = \det(tA - A^T)$$

where A *is any Seifert matrix for a* ***connected*** *Seifert surface.*

We refer to [Lic] for a proof. Note that the Alexander polynomial is only defined up to units of $\mathbb{Z}[t, t^{-1}]$, that is, up to a sign and multiplication by $t^{\pm 1}$. To remedy this ambiguity, we extend the ring to $\mathbb{Z}[t^{1/2}, t^{-1/2}]$ and make the following choice of normalization.

Definition 1.14. The **Conway-normalized Alexander polynomial** of L is

$$\Delta_L(t^{1/2}) = \det(t^{1/2}A - t^{-1/2}A^T)$$

where A is any Seifert matrix for a *connected* Seifert surface.

To show that the Conway-normalized Alexander polynomial is well-defined (not just up to units) one can again use S-equivalence, see [Lic]. Note also that

$$\det(t^{1/2}A - t^{-1/2}A^T) = t^{-|A|/2}\det(tA - A^T)$$

so the Conway-normalized Alexander polynomial is equivalent to the Alexander polynomial up to units in the ring $\mathbb{Z}[t^{1/2}, t^{-1/2}]$.

As with the Levine-Tristram signature, the (Conway-normalized) Alexander polynomial behaves well under basic operations on links. The properties in the following proposition are used Chapter 3.

Proposition 1.15. *Let L be a link. The (Conway-normalized) Alexander polynomial satisfies the following:*

1. *Symmetric under reciprocation:* $\Delta_L(t) = \Delta_L(t^{-1})$
2. *Invariance under orientation reversal:* $\Delta_L(t) = \Delta_{rL}(t)$
3. *Zero on disjoint unions:* $\Delta_{L' \sqcup L''}(t) = 0$
4. *Multiplicative under connected sum:* $\Delta_{L' \# L''}(t) = \Delta_{L'}(t)\Delta_{L''}(t)$ *where* $L' \# L''$ *denotes a link obtained by performing a connected sum between any component of* L' *and any component of* L''

Proof. The first assertion is immediate by Definition 1.14 since determinant of a matrix is the same as that of its transpose. The remaining arguments are similar to those of Proposition 1.10. □

We conclude by noting the relationship between the Alexander polynomial and the Levine-Tristram signature, though this relationship does not feature prominently in the remainder of this thesis. Since

$$(1-\omega)A + (1-\overline{\omega})A^T = -(1-\overline{\omega})(\omega A - A^T)$$

we see that $(1-\omega)A + (1-\overline{\omega})A^T$ is nonsingular exactly when the Alexander polynomial is nonzero. When ω is not a root of the Alexander polynomial, the Levine-Tristram signature is an integer-valued continuous function and therefore must be constant. Thus the roots of the Alexander polynomial are precisely where the Levine-Tristram signature can change value.

2 KASHAEV'S INVARIANT

In this chapter we introduce Kashaev's matrix and invariant, which were first defined in [Kas21].

An oriented link diagram D has the structure of a degree-4 planar graph by viewing the crossings of the diagram as the vertices of the graph. The **faces** and **vertices** of D are its faces and vertices as a planar graph; the term vertex is used in place of the term crossing to emphasize this perspective.

Definition 2.1. Given an oriented link diagram D, the **Kashaev matrix** τ_D is the $\mathbb{Z}[x]$-valued symmetric matrix with rows and columns indexed by the faces of D given by the following sum over the vertices of D:

$$\tau_D := \sum_v \operatorname{sgn}(v)\tau_v$$

where $\operatorname{sgn}(v) = \pm 1$ is the sign of v and τ_v is the matrix which is zero everywhere except in the 4×4 minor corresponding to the faces adjacent to v, where its values are in Figure 2.1.

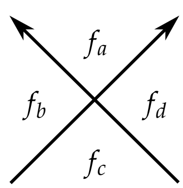

	f_a	f_b	f_c	f_d
f_a	$2x^2-1$	x	1	x
f_b	x	1	x	1
f_c	1	x	$2x^2-1$	x
f_d	x	1	x	1

Figure 2.1: A vertex v and its four adjacent faces, along with the corresponding 4×4 minor of τ_v.

If two of the surrounding faces of v are actually the same face, as in the vertex between f_2, f_5 and f_6 in Figure 2.2, then τ_v is nonzero in a 3×3 minor and the values of the shared face are given by summing the corresponding values of the two surrounding faces as if they were distinct.

Remark 2.2. The matrix τ_D actually has entries in $\mathbb{Z}[2x]$. To see this, notice that the only occurrences of x are in entries corresponding to two faces that share an edge, or in entries on the diagonal corresponding to a face with itself. Two faces that share an edge can only be adjacent to a common vertex by being on the two sides of a common edge, but for each edge

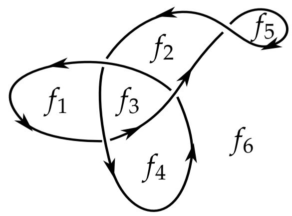

	f_1	f_2	f_3	f_4	f_5	f_6
f_1	$4x^2-2$	1	$2x$	1	0	$2x$
f_2	1	$4x^2-3$	$2x$	1	-1	0
f_3	$2x$	$2x$	3	$2x$	0	3
f_4	1	1	$2x$	$4x^2-2$	0	$2x$
f_5	0	-1	0	0	-1	$-2x$
f_6	$2x$	0	3	$2x$	$-2x$	$-4x^2+3$

Figure 2.2: An example of a diagram D and its Kashaev matrix τ_D

that they share, the vertices at the two endpoints will contribute a total of either zero or $\pm 2x$ to τ_D. As for the entries corresponding to a face with itself, the occurrences of x come from faces appearing near a vertex in the position of f_a or f_c in Figure 2.1. But any face appears as f_a the same number of times as it appears as f_c, and the contribution to τ_D from a single appearance of the pair f_a and f_c is $\pm 2(2x^2-1) = \pm((2x)^2-2)$.

While τ_D is not an invariant of links, its signature after a correction by the **writhe** (the sum of the signs of the crossings) is. The following theorem is due to Kashaev.

Theorem 2.3 (Kashaev [Kas21]). *Let L be an oriented link represented by the diagram D, and let wr_D denote the writhe of D. For any real value of x,*

$$\mathrm{sign}(\tau_D) - \mathrm{wr}_D$$

is an invariant of L.

The proof of Theorem 2.3 in [Kas21] uses a modified notion of S-equivalence to show invariance and requires $x \neq -\frac{1}{2}$. The interpretation in the proof of Theorem 3.1 makes clear that $\mathrm{sign}(\tau_D) - \mathrm{wr}_D$ computes the Levine-Tristram signature when $x \in (-1, 1)$, and is therefore an invariant for all real x.

3

MAIN RESULTS

In this chapter we prove Kashaev's conjecture and obtain as a corollary another formula for the Alexander polynomial. We end with a discussion of the kernel of the Kashaev matrix and its relationship to the Alexander module. The content of this chapter is based on [Liu25].

3.1 THE KASHAEV MATRIX TO THE LEVINE-TRISTRAM SIGNATURE

This section is dedicated to the proof of Kashaev's conjecture, wherein we construct Kashaev's matrix from the Seifert surface definition of the Levine-Tristram signature.

Theorem 3.1 (Kashaev's conjecture for signatures)**.** *Let L be an oriented link represented by a diagram D. The Levine-Tristram signature σ_L satisfies*

$$\sigma_L(\omega) = \frac{1}{2}(\operatorname{sign}(\tau_D) - \mathrm{wr}_D)$$

under the identification $2x = \sqrt{\omega} + \overline{\sqrt{\omega}} = 2\,\mathrm{Re}(\sqrt{\omega})$ for all $\omega \in S^1 \setminus \{1\}$.

The structure of the proof is as follows. Construct a particular Seifert surface for $L \sqcup rL$ whose first homology is generated by classes of curves corresponding to the faces and vertices of D. Using a Seifert matrix A with respect to these generators, we see that $Q = (1-\omega)A + (1-\overline{\omega})A^T$ is congruent to a block diagonal matrix with two blocks where one block corresponds to vertices and has signature $-\mathrm{wr}(D)$ and the other block corresponds to faces and, with a scaling of the generators, is exactly τ_D. Since $\operatorname{sign}(Q) = \sigma_{L \sqcup rL} = 2\sigma_L$, the proof is complete.

Proof. Following the outline above, we start by constructing a particular Seifert surface Σ for $L \sqcup rL$ starting from the diagram D of L:

1. At each crossing of D, draw a corresponding crossing for rL a bit "above and behind" the existing crossing in D, as in Figure 3.1.

2. Connect the new crossings with edges that follow along the corresponding edges in D, possibly creating an extra crossing between L and rL along each edge of D, to construct a diagram for $L \sqcup rL$. See Figure 3.2 for an example.

(a) A positive crossing (b) A negative crossing

Figure 3.1: A crossing of D (black) with the corresponding crossing (grey) for rL.

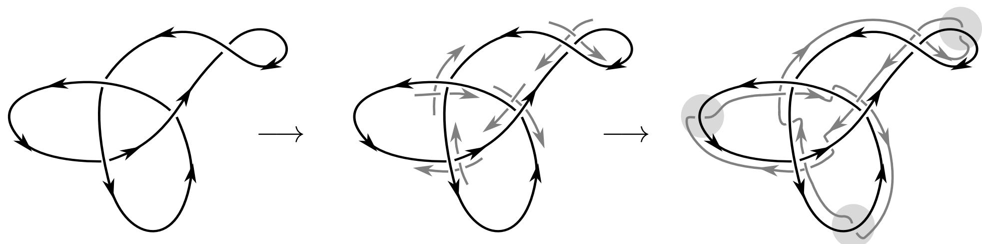

Figure 3.2: A diagram for a trefoil L and the corresponding diagram for $L \sqcup rL$. Three extra crossings occur along the edges of the original diagram, highlighted in light grey.

3. Apply Seifert's algorithm (see Definition 1.4) to the resulting diagram of $L \sqcup rL$ to get the Seifert surface Σ for $L \sqcup rL$.

The faces and vertices of D correspond to a set of generators for $H_1(\Sigma)$ since Σ deformation retracts onto a copy of D where each vertex is replaced by a circle, as in Figure 3.3.

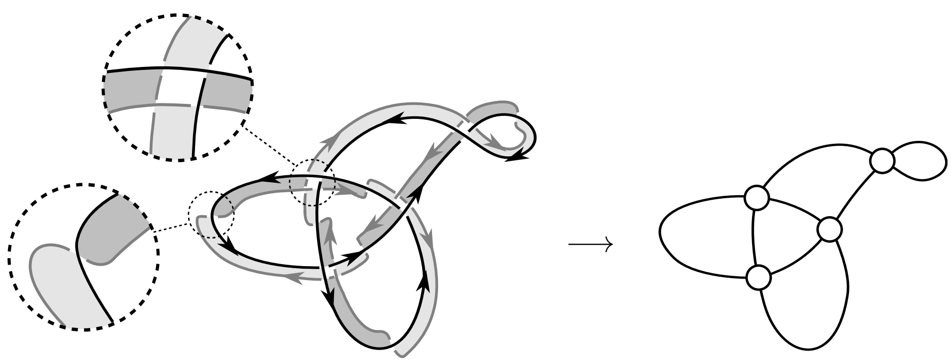

Figure 3.3: A Seifert surface for $L \sqcup rL$ which deformation retracts onto a diagram L whose vertices are replaced by circles.

Let A be a Seifert matrix with respect to this set of generators. Near a vertex of D there are five homology classes: one for each surrounding face and one for the vertex. We consider all five at once using a single picture as in Figure 3.4, where some segments in the picture are viewed as parts of different homology classes depending on the context. For example, in Figure 3.4 the top edge of the square in 3.4a can be viewed as a part of the curve corresponding to the upper face (3.4b) or as a part of the curve corresponding to the vertex (3.4c).

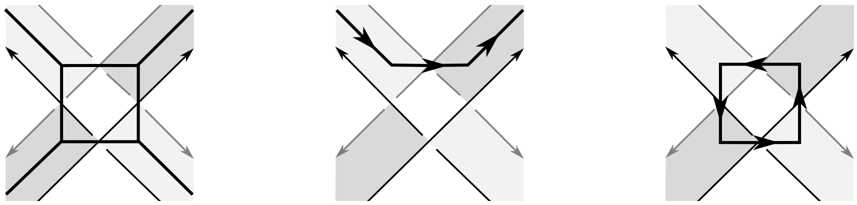

(a) The five homology curves near a vertex represented in one picture

(b) A curve representing the homology class corresponding to the upper face

(c) A curve representing the homology class corresponding to the vertex

Figure 3.4: The homology classes (thick black) near a positive vertex of D.

Using the convention that all curves generating $H_1(\Sigma)$ are oriented counterclockwise in the diagram, we compute the local contribution to the Seifert matrix A near each vertex of D, see Figure 3.5.

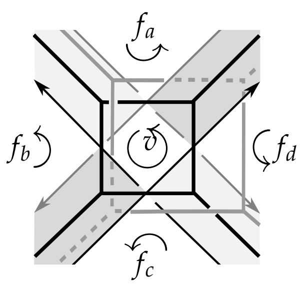

lk	f_a	f_b	f_c	f_d	v
$i^-(f_a)$	$-1/2$	0	0	$1/2$	0
$i^-(f_b)$	$-1/2$	0	$-1/2$	0	1
$i^-(f_c)$	0	0	$-1/2$	$1/2$	0
$i^-(f_d)$	0	0	0	0	0
$i^-(v)$	1	0	1	-1	-1

(a) Contribution to A near a positive vertex

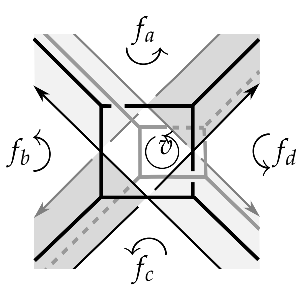

lk	f_a	f_b	f_c	f_d	v
$i^-(f_a)$	$1/2$	0	0	$1/2$	-1
$i^-(f_b)$	$-1/2$	0	$-1/2$	0	1
$i^-(f_c)$	0	0	$1/2$	$1/2$	-1
$i^-(f_d)$	0	0	0	0	0
$i^-(v)$	0	0	0	-1	1

(b) Contribution to A near a negative vertex

Figure 3.5: Contribution to a Seifert matrix A near a vertex of D. The lighter grey side of the surface in the figure corresponds to the negative pushoff direction.

Away from the vertices of D, such as near the border of the diagrams in Figure 3.5, we need to pick a side of the homology curve to draw the pushout on; an inconsistent choice would lead to an incorrect computation of total linking. We use the following convention: If the positive side of the surface is visible, the pushout is drawn between the homology curve and the original diagram for L, and if the negative side of the surface is visible, the pushout is drawn between the homology curve and the diagram for rL. This choice of convention is not arbitrary: it is specifically chosen to ensure that no linking occurs near the crossings of $L \sqcup rL$ occurring along the edges of D, see Figure 3.6.

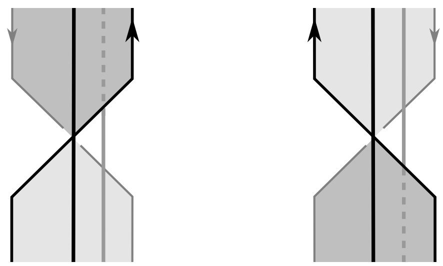

Figure 3.6: A positive (left) and negative (right) crossing of $L \sqcup rL$ along the edge of D. No linking occurs between the homology curves (black) and the pushouts (grey).

Using this drawing convention, the only linking occurs near the vertices of D, so we can compute the Seifert matrix A by summing the local contributions to linking number given by Figure 3.5 over the vertices of D. Note that the homology curve corresponding to a vertex has zero linking with the pushout of a curve corresponding to a different vertex, so the matrix $Q = (1-\omega)A + (1-\overline{\omega})A^T$ has the following form:

$$Q = \begin{array}{c||c|c} & \text{faces} & \text{vertices} \\ \hline\hline \text{faces} & X & Y \\ \hline \text{vertices} & Y^* & Z \end{array}$$

where Z is a diagonal matrix with $-(1-\omega)-(1-\overline{\omega})$ in the entries corresponding to positive vertices and $1-\omega+1-\overline{\omega}$ in the entries corresponding to negative vertices. In particular, Z is invertible and satisfies $\operatorname{sign}(Z) = -\operatorname{wr}(D)$. Observe that Q is congruent to the block diagonal matrix

$$MQM^* = \begin{pmatrix} X - YZ^{-1}Y^* & 0 \\ 0 & Z^{-1} \end{pmatrix}$$

via the matrix

$$M = \begin{pmatrix} I & -YZ^{-1} \\ 0 & Z^{-1} \end{pmatrix}.$$

As congruent matrices have the same signature and $\operatorname{sign}(Q) = 2\sigma_L$, it remains to show that

$$\operatorname{sign}(X - YZ^{-1}Y^*) = \operatorname{sign}(\tau_D)\,.$$

We show that $X - YZ^{-1}Y^*$ is exactly equal to τ_D under an appropriate scaling of the generators. Make the following computation

$$(YZ^{-1}Y^*)_{i,j} = \sum_{k,\ell} Y_{i,k}(Z^{-1})_{k,\ell}(Y^*)_{\ell,j} = \sum_k Y_{i,k}Z^{-1}_{k,k}\overline{Y_{j,k}}$$

and notice that it's only possible for both $Y_{i,k}$ and $Y_{j,k}$ to be nonzero if faces i and j are both adjacent to vertex k. Therefore $YZ^{-1}Y^*$ is a sum over vertices, where the contribution at each vertex is a matrix that is zero everywhere except in the 4×4 minor corresponding to the four adjacent faces of the vertex. The same is then true for $X - YZ^{-1}Y^*$, and the 4×4 minor of the contribution to $X - YZ^{-1}X^*$ at each vertex is given by performing the same matrix operations to the local contribution to Q. We show the explicit computation for this 4×4 minor below; the result is in Figure 3.7.

Writing the contribution to A from Figure 3.5 heuristically as

lk	f	v
$i^-(f)$	α	β
$i^-(v)$	γ	δ

where α is a 4×4 block and δ is a 1×1 block, and using the substitution

$$s = 1 - \omega$$

we can write the local contribution to $Q = sA + \bar{s}A^T$ as follows:

	$\bar{f}$	$\bar{v}$
f	$s\alpha + \bar{s}\alpha^T$	$s\beta + \bar{s}\gamma^T$
c	$s\gamma + \bar{s}\beta^T$	$(s + \bar{s})\delta$

where the notation $\bar{f}$ and $\bar{v}$ in the top row reminds us that when viewed as a Hermitian form, Q is conjugate linear in the second component. The local contribution to $X - YZ^{-1}Y^*$ is therefore

$$(s\alpha + \bar{s}\alpha^T) - (s\beta + \bar{s}\gamma^T)((s+\bar{s})\delta)^{-1}(s\gamma + \bar{s}\beta^T)$$

which, noting that $s + \bar{s} = s\bar{s}$ and $s\overline{\omega} = -\bar{s}$, simplifies to

$$s\alpha + \bar{s}\alpha^T - (\beta - \overline{\omega}\gamma^T)\delta^{-1}(\beta^T - \omega\gamma)\,.$$

This local contribution to $X - YZ^{-1}Y^*$ is given explicitly in Figure 3.7 by substituting the values for α, β, γ, and δ from Figure 3.5.

$$\begin{array}{c|c}
(+) & \begin{array}{cccc} \bar{f}_a & \bar{f}_b & \bar{f}_c & \bar{f}_d \end{array} \\
\hline
\begin{array}{c} f_a \\ f_b \\ f_c \\ f_d \end{array} &
\begin{bmatrix}
\frac{\omega+\overline{\omega}}{2} & -\frac{1+\overline{\omega}}{2} & 1 & -\frac{1+\omega}{2} \\
-\frac{1+\omega}{2} & 1 & -\frac{1+\omega}{2} & \omega \\
1 & -\frac{1+\overline{\omega}}{2} & \frac{\omega+\overline{\omega}}{2} & -\frac{1+\omega}{2} \\
-\frac{1+\overline{\omega}}{2} & \overline{\omega} & -\frac{1+\overline{\omega}}{2} & 1
\end{bmatrix}
\end{array}
\qquad
\begin{array}{c|c}
(-) & \begin{array}{cccc} \bar{f}_a & \bar{f}_b & \bar{f}_c & \bar{f}_d \end{array} \\
\hline
\begin{array}{c} f_a \\ f_b \\ f_c \\ f_d \end{array} &
\begin{bmatrix}
-\frac{\omega+\overline{\omega}}{2} & \frac{1+\overline{\omega}}{2} & -1 & \frac{1+\omega}{2} \\
\frac{1+\omega}{2} & -1 & \frac{1+\omega}{2} & -\omega \\
-1 & \frac{1+\overline{\omega}}{2} & -\frac{\omega+\overline{\omega}}{2} & \frac{1+\omega}{2} \\
\frac{1+\overline{\omega}}{2} & -\overline{\omega} & \frac{1+\overline{\omega}}{2} & -1
\end{bmatrix}
\end{array}$$

Figure 3.7: The local contribution to $X - YZ^{-1}Y^*$ of a positive vertex (left) and negative vertex (right).

The local contributions to $X - YZ^{-1}Y^*$ in Figure 3.7 are precisely the local contributions to τ_D from Figure 2.1 after scaling the faces in the following way. Let the winding of a face in D be the winding number of D around any point in that face. Extend the coefficient ring to $\mathbb{Z}[\sqrt{\omega}^{\pm 1}]$ and for a face f with winding k use the generator $(-\overline{\sqrt{\omega}})^k f$ in place of f. Note that it's fine to extend the ring in this way since the signature is ultimately taken over $\mathbb{C}$ for any particular choice of ω. This multiplies each row of $X - YZ^{-1}Y^*$ by some $(-\overline{\sqrt{\omega}})^k$ and the corresponding column by the complex conjugate $(-\sqrt{\omega})^k = (-\overline{\sqrt{\omega}})^{-k}$. The matrices in Figure 3.7 are then exactly the ones in Figure 2.1 under the identification $2x = \sqrt{\omega} + \overline{\sqrt{\omega}}$, so $X - YZ^{-1}Y^*$ becomes exactly τ_D. Since this scaling preserves the signature, $\operatorname{sign}(X - YZ^{-1}Y^*) = \operatorname{sign}(\tau_D)$.

□

Remark 3.2. Note that Theorem 3.1 does not give an interpretation of Kashaev's invariant when $x \notin [-1, 1)$. Computational evidence suggests that Kashaev's invariant is always zero outside of this range but we do not know why.

3.2 THE KASHAEV SIGNATURE TO THE ALEXANDER POLYNOMIAL

The relationship between Kashaev's matrix and the Alexander polynomial appeared in [CF24], was independently noticed by Dror Bar-Natan, and was the inspiration behind the main ideas in the proof of Theorem 3.1. In this section we present an alternative proof of this result following these ideas.

Theorem 3.3. *Let D be a diagram for an oriented link L. Let f_i and f_j be two faces in D that share an edge, and let $\widetilde{\tau}_D$ be the Kashaev matrix τ_D with the two columns and rows corresponding to f_i and f_j removed. The Conway-normalized Aexander polynomial Δ_L satisfies*

$$\Delta_L(t)^2 = \det(\widetilde{\tau}_D)$$

under the identification $2x = t^{1/2} + t^{-1/2}$.

Proof. The proof is similar to that of Theorem 3.1, but consider in place of $L \sqcup rL$ a connected sum $L\#rL$ taken between the component of L that the shared edge between f_i and f_j belongs to and its corresponding component of rL. Use the same procedure as in the proof of Theorem 3.1 to construct a diagram and Seifert surface $\Sigma_\#$ for $L\#rL$, drawing the connected sum along the shared edge of f_i and f_j, see Figure 3.8.

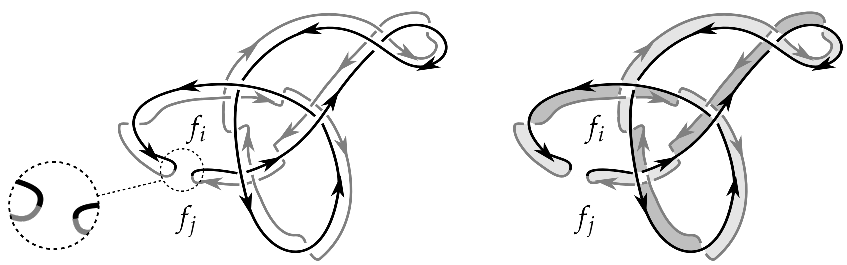

Figure 3.8: A diagram and Seifert surface for $L\#rL$ with the connected sum along the shared edge of f_i and f_j.

There is a linearly independent basis for $H_1(\Sigma_\#)$ corresponding to the vertices and faces of D with f_i and f_j excluded. Let A be a Seifert matrix for $\Sigma_\#$ with respect to this basis. Note that A is simply the Seifert matrix for $L \sqcup rL$ from the proof of Theorem 3.1, but with the two rows and columns corresponding to f_i and f_j removed. Now consider the matrix

$$Q = (1-t)A + (1-t^{-1})A^T$$

over the involutive ring $\mathbb{Z}[t^{\pm 1/2}]$ with involution given by $t^{1/2} \mapsto t^{-1/2}$. As in the proof of Theorem 3.1, the matrix Q has the following form:

$$Q = \begin{array}{c||c|c} & \text{faces except } \{f_i, f_j\} & \text{vertices} \\ \hline\hline \text{faces except } \{f_i, f_j\} & X & Y \\ \hline \text{vertices} & Y^* & Z \end{array}$$

where the notation Y^* denotes the transpose of Y under the involution $t \mapsto t^{-1}$ so that when t is a unit complex number, Y^* is the usual conjugate transpose. Note that Z is diagonal with $-((1-t)+(1-t^{-1}))$ in the entries corresponding to positive vertices and $(1-t)+(1-t^{-1})$ in the entries corresponding to negative vertices. Working over the localized ring $\mathbb{Z}[t^{\pm 1/2}, (1-t)^{-1}]$ so that Z is invertible, notice that

$$MQM^* = \begin{pmatrix} X - YZ^{-1}Y^* & 0 \\ 0 & Z^{-1} \end{pmatrix}$$

where $M = \begin{pmatrix} I & -YZ^{-1} \\ 0 & Z^{-1} \end{pmatrix}$. Therefore

$$\begin{aligned} \det(Q) &= \det(X - YZ^{-1}Y^*) \det(Z^{-1}) \det(M)^{-1} \det(M^*)^{-1} \\ &= \det(X - YZ^{-1}Y^*) \det(Z) \\ &= (-1)^p ((1-t)+(1-t^{-1}))^{|V_D|} \det(X - YZ^{-1}Y^*) \end{aligned}$$

where p is the number of positive vertices in D and $|V_D|$ is the total number of vertices in D. To change $X - YZ^{-1}Y^*$ into $\widetilde{\tau}_D$ we multiply each row by some $(-t^{1/2})^k$ and the corresponding column by $(-t^{-1/2})^{-k}$ so the determinant is preserved. We can also rewrite $(1-t)+(1-t^{-1})$ as $-(t^{1/2}-t^{-1/2})^2$, so we get

$$\det(Q) = (-1)^{p+|V_D|} (t^{1/2} - t^{-1/2})^{2|V_D|} \det(\widetilde{\tau}_D)$$

Finally, notice that

$$Q = (t^{-1/2} - t^{1/2})(t^{1/2}A - t^{-1/2}A^T)$$

and use the definition of the Conway-normalized Alexander polynomial to get

$$\begin{aligned} \Delta_{L\#-L}(t^{1/2}) &= \det(t^{1/2}A - t^{-1/2}A^T) \\ &= (t^{-1/2} - t^{1/2})^{-2|V_D|} \det(Q) \\ &= (-1)^{p+|V_D|} \det(\widetilde{\tau}_D) \end{aligned}$$

Since $\Delta_{L\#rL} = \Delta_L^2$, this concludes the proof. □

Corollary 3.4. *We can also use $\widetilde{\tau}_D$ to compute σ_L. That is,*

$$\sigma_L(\omega) = \frac{1}{2}(\operatorname{sign}(\widetilde{\tau}_D) - \mathrm{wr}_D)$$

Proof. Since $\sigma_{L\#rL} = \sigma_{L\sqcup rL}$ we can use $L\#rL$ instead of $L \sqcup rL$ in the proof of Theorem 3.1. □

Remark 3.5. Corollary 3.3 does not determine the sign of the Conway-normalized Alexander polynomial since there is a square in the equation.

Remark 3.6. We used an explicit formula for the Conway-normalized Alexander polynomial in Corollary 3.3 to show its relationship to $\det(\tilde{\tau}_D)$, but showing that $\det(\tilde{\tau}_D)$ gives *any* Alexander polynomial would be enough to show that it gives the Conway-normalized one (up to sign): indeed, since $\tilde{\tau}_D$ is a real matrix when $t \in S^1$, it must be symmetric under $t \mapsto t^{-1}$.

Remark 3.7. The proof of Corollary 3.3 allows us to describe $\tilde{\tau}_D$ as a presentation matrix of the Alexander module of L over the localized ring $\mathbb{Z}[t^{\pm 1/2}, (1-t)^{-1}]$ under the substitution $2x = t^{1/2} + t^{-1/2}$. If L is a knot, multiplication by $1-t$ is invertible in the Alexander module so $\tilde{\tau}_D$ also presents the Alexander module over $\mathbb{Z}[t^{\pm 1/2}]$. Note that this does *not* describe the $\mathbb{Z}[2x]$-module that τ_D presents, or even show that this module is an invariant of links.

3.3 THE KERNEL OF THE KASHAEV MATRIX

We conclude this chapter with explicit formulas for the kernel of the Kashaev matrix τ_D. We can view τ_D either as a linear map or as a symmetric bilinear form $\langle \cdot, \cdot \rangle_D$ on the $\mathbb{Z}[2x]$-module freely generated by the faces F_D of D, where $\langle f_i, f_j \rangle = (\tau_D)_{i,j}$. The kernel of τ_D as a linear map is the same as its kernel as a symmetric bilinear form. The corollaries in this section give explicit formulas for this kernel, though we do not know a topological interpretation for these results.

Corollary 3.8. *The kernel of τ_D contains the 2-dimensional submodule generated by*

$$\sum_{f \in F_D} a_{w(f)} f$$

where $w(f)$ is the number of times the diagram winds around a point in the face f, and the coefficients a_n are solutions to the recurrence relation $a_n + 2x a_{n+1} + a_{n+2} = 0$. If we use the identification $2x = t^{1/2} + t^{-1/2}$ and consider τ_D over the field $\mathbb{Q}(t^{1/2})$, then this subspace is the entire kernel if $\Delta_L(t) \neq 0$. Furthermore, the solutions to this recurrence are given explicitly by

$$a_n = c_1(-t^{1/2})^n + c_2(-t^{-1/2})^n$$

for constants $c_1, c_2 \in \mathbb{Q}(t^{1/2})$.

Proof. We first verify that $g = \sum_{f \in F_D} a_{w(f)} f$ lives in the kernel of the symmetric bilinear form $\langle \cdot, \cdot \rangle_D$ represented by τ_D. Consider $\langle g, f \rangle_D$ for an arbitrary face f, and recall the local contributions in the definition of τ_D from Figure 2.1, copied below.

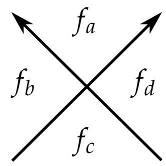

	f_a	f_b	f_c	f_d
f_a	$2x^2-1$	x	1	x
f_b	x	1	x	1
f_c	1	x	$2x^2-1$	x
f_d	x	1	x	1

If f appears as f_b in the diagram above near some vertex and $w(f) = k$, then $w(f_a) = w(f_c) = k-1$ and $w(f_d) = k-2$, so the contribution to $\langle g, f \rangle_D$ of this vertex is

$$\begin{aligned} & a_k \langle f_b, f_b \rangle_D + a_{k-1} \langle f_b, f_a \rangle_D + a_{k-1} \langle f_b, f_c \rangle_D + a_{k-2} \langle f_b, f_d \rangle_D \\ =& a_k + 2x a_{k-1} + a_{k-2} \\ =& 0 \end{aligned}$$

A similar computation shows that the contribution is also zero when f appears in position f_a, f_c, or f_d, hence g is in the kernel of τ_D. The submodule is 2-dimensional since the solution space to $a_n + 2x a_{n+1} + a_{n+2} = 0$ is 2-dimensional. The proof of Corollary 3.3 shows that the kernel of τ_D is 2-dimensional when $\Delta_L \neq 0$, so over a field this is the entire kernel. It is straightforward to verify that the explicit expression of a_n gives solutions to the recurrence.

□

If D is disconnected then the Alexander polynomial is always zero and the kernel is larger. We can extend Corollary 3.8 to give a more general result.

Corollary 3.9. *Let D be a diagram with n connected components $D_1, \cdots, D_n$. Let f_0 be the exterior face and let F'_{D_i} be the set of* ***interior*** *faces of D_i. The kernel of τ_D contains the $n+1$-dimensional subspace generated by*

$$a_0 f_0 + \sum_{i=1}^{n} \sum_{f \in F'_{D_i}} a_{i,w(f)} f$$

where each sequence $\{a_{i,k}\}_{k \in \mathbb{Z}}$ satisfies the recurrence relation $a_{i,k} + 2x a_{i,k+1} + a_{i,k+2} = 0$ with the condition $a_{i,0} = a_0$ for all i. If none of the Alexander polynomials $\Delta_{L_i}(t)$ are zero, where L_i is the link represented by D_i, then over the field $\mathbb{Q}(t^{1/2})$ this is the entire kernel.

Proof. The computations in the proof of Corollary 3.8, along with the observation that interior faces of different diagrams don't share vertices, show that the subspace is indeed in the kernel. The solution space to the recurrence is $n+1$ dimensional, so it remains to show that the kernel of τ_D has dimension $n+1$ when all the Δ_{L_i} are nonzero. Using a similar procedure as in the proof of Corollary 3.3, pick one face in each F'_{D_i} that shares an edge with f_0, and let $\widetilde{\tau}_D$ be τ_D with the $n+1$ rows and columns corresponding to these faces and f_0 removed. Let A_i be a Seifert matrix for $L_i \# r L_i$ so that the block diagonal matrix with $tA_i - A_i^T$ in each block has determinant $\prod_{i=1}^{n} \Delta_{L_i}$. As in the proof of Corollary 3.3, we can get to $\widetilde{\tau}_D$ from this block diagonal matrix without changing the determinant, so if each Δ_{L_i} is nonzero, $\widetilde{\tau}_D$ has full rank and the kernel of τ_D has dimension $n+1$.

□

A

APPENDIX

The results from Chapter 3 generalize to the multivariable signature and multivariable Alexander polynomial for coloured links. In this section we introduce the necessary background and state without proof the analogous results to Theorem 3.1 and Corollary 3.3. This generalization is due to joint work of the author with Cimasoni and Ferretti [CFL25], and is not a part of this thesis.

Given an integer $\mu > 0$, a **μ-coloured link** is an oriented link $L = L_1 \cup \cdots \cup L_\mu$ such that each component is assigned a colour in $\{1, \ldots, \mu\}$ and L_i denotes the sublink consisting of all components of colour i. Two coloured links are equivalent if they are related by an ambient isotopy which preserves the orientation and colour of all components.

The strands in a **coloured diagram**, a link diagram for a coloured link, has coloured strands. A crossing in a coloured diagram is **monochromatic** if the two strands of the crossing have the same colour, and **bichromatic** otherwise.

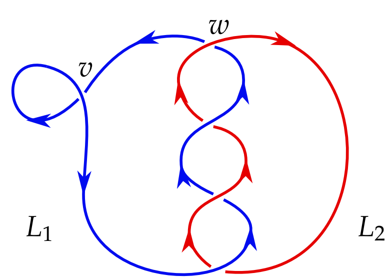

Figure A.1: A coloured diagram for a 2-colored link $L = L_1 \cup L_2$. The crossing v is monochromatic and w is bichromatic.

As the single variable Alexander polynomial and Levine-Tristram signature can be defined using Seifert surfaces, their multivariable generalizations can be defined using generalized Seifert surfaces, known as C-complexes.

Definition A.1. A **C-complex** for a μ-coloured link $L = L_1 \cup \cdots \cup L_\mu$ is a union $S = S_1 \cup \cdots \cup S_\mu$ of surfaces embedded in S^3 satisfying the following conditions:

1. For all i, the surface S_i is a Seifert surface for L_i.

2. For all $i \neq j$, the surfaces S_i and S_j intersect in a finite number of **clasps**, see Figure A.2.

Figure A.2: A **positive** (+1) clasp (left) and a **negative** (-1) clasp (right).

3. For all i, j, k pairwise distinct, the intersection $S_i \cap S_j \cap S_k$ is empty.

If $\mu = 1$, a C-complex is a Seifert surface. The properties of Seifert surfaces discussed in Chapter 1 generalize to C-complexes, including the notions of Seifert forms and matrices.

Definition A.2. Given a C-complex S and a choice of signs $\varepsilon = (\varepsilon_1, \dots, \varepsilon_\mu) \in \{\pm 1\}^\mu$, there is a bilinear form

$$\alpha^\varepsilon \colon H_1(S) \times H_1(S) \longrightarrow \mathbb{Z}$$

given by $\alpha^\varepsilon(a, b) = \mathrm{lk}(a^\varepsilon, b)$ on primitive classes and extending linearly to all of $H_1(S)$, where a^ε denotes a pushoff of a from S_i in the ε_i-normal direction. A **generalized Seifert matrix** A^ε is a matrix that represents α^ε.

Note that the generalized Seifert matrices A^-, A^+ of a 1-coloured link coincide with a usual Seifert matrix A and its transpose A^{T}. Both the multivariable signature and Alexander polynomial can be computed using generalized Seifert matrices. As in the single variable case, there is a normalization of the multivariable Alexander polynomial in the ring $\Lambda_\mu = \mathbb{Z}[t_1^{\pm 1/2}, \cdots, t_\mu^{\pm 1/2}]$ called the Conway function which we introduce instead.

For the remainder of this chapter, let $L = L_1 \cup \cdots \cup L_\mu$ be a μ-coloured link with diagram D and let $S = S_1 \cup \cdots S_\mu$ be a C-complex for L with generalized Seifert matrix A^ϵ.

Definition A.3. The **(multivariable) signature** of L is the function $\sigma_L : (S^1 \setminus \{1\})^\mu \to \mathbb{Z}$ given by

$$\sigma_L(\omega_1, \cdots, \omega_\mu) = \mathrm{sign}(H(\omega)), \text{ where } H(\omega) = \sum_{\varepsilon \in \{\pm 1\}^\mu} \left(\prod_{i=1}^{\mu} (1 - \overline{\omega}_i^{\varepsilon_i}) \right) A^\varepsilon .$$

Definition A.4. If S is a *connected* C-complex, then the **Conway function** of L is the polynomial in the ring Λ_μ given by

$$\nabla_L(t_1^{1/2}, \cdots, t_\mu^{1/2}) = \operatorname{sgn}(S)\rho \det(A_S)\,, \text{ where } \begin{cases} \operatorname{sgn}(S) \text{ is the product of the signs} \\ \qquad\qquad \text{of the clasps of } S \\ \rho = \prod_{i=1}^{\mu} (t_i^{1/2} - t_i^{-1/2})^{\chi(S \setminus S_i)-1} \\ A_S = \sum_{\varepsilon \in \{\pm 1\}^\mu} \left(\prod_{i=1}^{\mu} \varepsilon_i t_i^{\varepsilon_i/2} \right) A^\varepsilon \end{cases}$$

These invariants are well defined and agree with the Levine-Tristram signature and the Conway-normalized Alexander polynomial when $\mu = 1$. To state multivariable versions of Theorem 3.1 and Corollary 3.3, it remains to introduce a multivariable analogue of Kashaev's matrix.

Definition A.5. Let $x = \{x_j, x_{jk} \mid 1 \leq j, k \leq \mu\}$ be formal variables indexed by (unordered pairs of) colours. The **(multivariable) Kashaev matrix** τ_D^μ is the symmetric matrix with rows and columns indexed by the faces of D given by the following sum over the vertices of D:

$$\tau_D^\mu = \sum_v \frac{\operatorname{sgn}(v)}{\sqrt{1 - x_j^2}\sqrt{1 - x_k^2}} \tau_v^\mu$$

where the indices $j, k \in \{1, \ldots, \mu\}$ are the (possibly identical) colours of the two strands crossing at v and τ_v^μ is zero except in the 4×4 minor corresponding to the faces adjacent to v, where its values are given in Figure A.3.

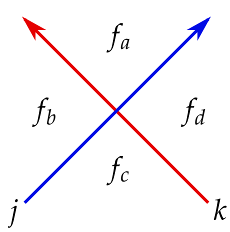

	f_a	f_b	f_c	f_d
f_a	x_{jk}	x_j	1	x_k
f_b	x_j	$2x_j x_k - x_{jk}$	x_k	1
f_c	1	x_k	x_{jk}	x_j
f_d	x_k	1	x_j	$2x_j x_k - x_{jk}$

Figure A.3: A crossing v and the corresponding 4×4 minor of τ_v^μ. The incoming left strand is of color j, the incoming right strand of colour k, and the four adjacent faces are f_a, f_b, f_c, and f_d.

As in the single variable case, if the faces f_a, f_b, f_c, f_d around a crossing v are not all distinct, we add the corresponding rows and columns of τ_v^μ.

Remark A.6. When $\mu = 1$, the multivariable Kashaev matrix τ_D^1 is *not* the single variable Kashaev matrix τ_D. In particular, τ_D^1 uses two formal variables x_1 and x_{11} instead of a single variable x as τ_D does. However, they do agree under the identifications with ω and t in Theorems A.0.7 and A.0.8.

Theorem A.0.7. *The multivariable signature σ_L can be computed by*

$$\sigma_L(\omega) = \tfrac{1}{2}(\operatorname{sign}(\tau_D^\mu) - \mathrm{wr}_D^{\mathrm{m}})$$

under the identification $x_j = \mathrm{Re}(\omega_j^{1/2})$ and $x_{jk} = \mathrm{Re}(\omega_j^{1/2}\omega_k^{1/2})$, where $\mathrm{wr}_D^{\mathrm{m}}$ denotes the sum of the signs of all monochromatic crossings of D.

Theorem A.0.8. *Suppose D is **connected**. Let f_i and f_j be two faces of D that share an edge of colour c. Let $\widetilde{\tau}_D^\mu$ be the matrix τ_D^μ with the two columns and rows corresponding to f_i and f_j removed. The Conway function ∇_L satisfies*

$$\nabla_L^2(t_1^{1/2}, \ldots, t_\mu^{1/2}) = \frac{\det(\widetilde{\tau}_D^\mu)}{(t_c^{1/2} - t_c^{-1/2})^2}\left(\prod_v -\operatorname{sgn}(v)\frac{t_j^{1/2} - t_j^{-1/2}}{2}\frac{t_k^{1/2} - t_k^{-1/2}}{2}\right)$$

where the product is over all vertices of D, the indices j, k are the (possibly identical) colours of the two strands crossing at v, and we use the identification

$$x_j = \frac{t_j^{1/2} + t_j^{-1/2}}{2}, \quad x_{jk} = \frac{t_j^{1/2}t_k^{1/2} + t_j^{-1/2}t_k^{-1/2}}{2}.$$

The proofs of Theorems A.0.7 and A.0.8 are largely the same as that of Theorem 3.1 and Corollary 3.3; the main differences are in constructing the C-complex and computing local linking near bichromatic crossings. Note also that Theorem A.0.7 holds true with $\widetilde{\tau}_D^\mu$ instead for the same reason as in Corollary 3.4. There are also results regarding the kernel and the multivariable Alexander module analogous to those at the end of Chapter 3, but we leave further discussions and the proofs of Theorems A.0.7 and A.0.8 to [CFL25].

BIBLIOGRAPHY

[CF24] David Cimasoni and Livio Ferretti, **On the Kashaev signature conjecture**, Fund. Math. **266** (2024), no. 3, 275–287. MR 4806171

[CFL25] David Cimasoni, Livio Ferretti, and Jessica Liu, **A diagrammatic computation of abelian link invariants**, Algebr. Geom. Topol. **in press.** (2025).

[Con21] Anthony Conway, **The Levine-Tristram signature: a survey**, 2019–20 MATRIX annals, MATRIX Book Ser., vol. 4, Springer, Cham, [2021] ©2021, pp. 31–56. MR 4294761

[Kas21] Rinat Kashaev, **On symmetric matrices associated with oriented link diagrams**, Topology and geometry—a collection of essays dedicated to Vladimir G. Turaev, IRMA Lect. Math. Theor. Phys., vol. 33, Eur. Math. Soc., Zürich, [2021] ©2021, pp. 131–145. MR 4394506

[Lic] W. B. Raymond Lickorish, **An introduction to knot theory**, Graduate Texts in Mathematics, vol. 175, Springer-Verlag, New York.

[Liu25] Jessica Liu, **A proof of the Kashaev signature conjecture**, Quantum Topol. **in press.** (2025).